

Effectiveness conditions of sodium monofluorophosphate as a corrosion inhibitor for concrete reinforcements

Thierry Chaussadent ^{a,*}, Véronique Nobel-Pujol ^a, Fabienne Farcas ^a,
Isabelle Mabilie ^b, Christian Fiaud ^b

^a *Laboratoire Central des Ponts des Chaussées, Physico-Chimie des Matériaux, 58 Boulevard Lefebvre, 75732, Paris Cedex 15, France*

^b *Laboratoire de Génie des Procédés Plasmas et Traitement de Surfaces, UPMC/ENSCP- EA 3492, Ecole Nationale Supérieure de Chimie de Paris, 11 rue Pierre et Marie Curie, 75231, Paris Cedex 05, France*

Received 4 April 2005; accepted 21 September 2005

Abstract

Among the array of protection and repair methods for reinforced concrete structures when steel reinforcements undergo corrosion, the use of migrating corrosion inhibitors could prove to be an attractive alternative. These products, applied to the concrete surface, are intended to diffuse into the concrete in order to reach the reinforcement and stop or delay corrosion.

Some key aspects on the use of monofluorophosphate (MFP) as an inhibitor for concrete reinforcements are presented first. The experimental work has focused on developing a method to determine the amount of MFP in concrete and on studying the chemical interactions taking place between MFP and certain concrete components. These data are then used to explain MFP penetration profiles in concretes as well as the correlation with electrochemical measurements.

© 2005 Elsevier Ltd. All rights reserved.

Keywords: Sodium monofluorophosphate; A. Reaction; C. Corrosion; C. Transport properties; C. Electrochemical properties

1. Introduction

Monofluorophosphate (MFP) has been used as a corrosion inhibitor for concrete reinforcements over the last 20 years. It is applied at the concrete surface in the form of an aqueous solution with a mass percentage ranging between 10% and 20%. The effectiveness of MFP, applied to the surface of a concrete structure, is based on both its diffusion into the concrete pore network and its action on steel reinforcement surface. Accordingly, the fundamental stage herein is the ease of access of MFP to the reinforcements.

It has often been mentioned in the literature [1–3] that in early-age concrete, the penetration of an aqueous MFP solution is insufficient or impossible and, as a consequence, the PO_3F^{2-} ions, which actually perform the inhibiting action, are not present in sufficient quantities within the interstitial solution to successfully inhibit corrosion. By forming apatites with Ca-

containing compounds when the concrete has not been carbonated, PO_3F^{2-} ions are trapped but reaction products may accumulate in some parts of the porous network, thus blocking the penetration of aggressive species. In a carbonated concrete, aqueous MFP solutions are better able to penetrate [2–4]. MFP penetration should occur by means of a pure diffusion process whenever the concrete is saturated. Other types of penetrations could also arise depending on the amount of water in the concrete pore network [4].

The work presented in this paper lies within the scope of a research programme [5] conducted on the effectiveness of MFP and focuses on the knowledge of MFP, in particular in terms of its potential penetration into concrete materials.

2. Materials and methods

2.1. Materials

Cylindrical mortar specimens (35 mm diameter and 40 mm long) containing a centred mild steel bar ($\text{C} \approx 0.16\%$ – $\text{Si} \approx 0.12\%$ and $\text{Mn} \approx 0.4\%$) (6 mm diameter) were cast with

* Corresponding author. Tel.: +33 1 40 43 50 00; fax: +33 1 40 43 65 14.
E-mail address: chaussadent@lcpc.fr (T. Chaussadent).

Table 1
Chemical composition of the cement and mix design of mortar specimens

| Cement composition | Mass % | Mortar composition | Kg/m ³ |
|--------------------------------|--------|--------------------|-------------------|
| SiO ₂ | 20.6 | Cement | 516 |
| Al ₂ O ₃ | 4.9 | Sand | 1504 |
| Fe ₂ O ₃ | 2.9 | Water | 258 (W/C=0.5) |
| CaO | 61.3 | | |
| MgO | 4.5 | | |
| K ₂ O | 1.16 | | |
| Na ₂ O | 0.24 | | |
| SO ₃ | 3.1 | | |
| Free CaO | 1.1 | | |
| LOI | 0.7 | | |

ordinary Portland cement. The compositions of both the cement and the mortar are listed in Table 1.

Cement paste specimens were also produced using Portland cement and a W/C ratio of 0.5. All specimens were wrapped in an adhesive aluminium sheet, in order to reduce moisture loss, and then conserved one year at 20 °C before the experimental campaign.

The purity of the MFP used, as determined by quantifying the phosphorus, was 96±3%. Prior to applications on cementitious specimen surfaces, an X-ray diffraction diagram of MFP was carried out to verify it had not been hydrolysed.

2.2. Methods

The method used for determining the MFP content in concrete has been previously presented in [6]. This method consists of the total dissolution of concrete in a 4% nitric acid solution, followed by determination of the MFP amount in the solution by means of ion chromatography (Dionex DX120 chromatograph).

As regards the electrochemical tests performed on an EG and G apparatus (Model 263A Potentiostat and Model 1025 Frequency Analyzer), the study focused on reinforced mortar specimens submitted or not to degradation (chloride ions, carbonation). Two electrochemical techniques were selected herein, i.e.:

- monitoring of steel corrosion potential over time; this technique, mainly used in situ to produce maps of the corrosion state, makes it possible to detect electrochemical “events” (more or less distinct variations in potential); and
- determination of electrochemical impedance spectroscopy (EIS) diagrams, a technique that has been used quite often [7–9] over the past few years yet one in which implementation for metal embedded in concrete, as well as in results interpretation, is not straightforward.

3. Experimental program and results

3.1. Interactions between MFP and concrete constituents

This first part of the study was devoted to the analysis of chemical interactions between MFP and some of the major

concrete constituents in order to define the penetration conditions of this inhibitor within concrete structures. As indicated previously, the main limiting factor is apatite formation. It thus appeared necessary to determine the apatite formation conditions. In pursuit of this objective, the study has been carried out to determine the following:

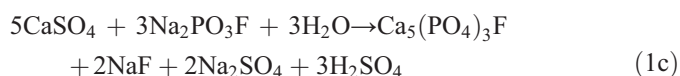
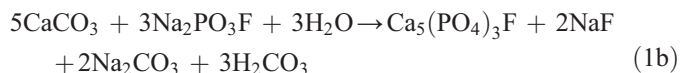
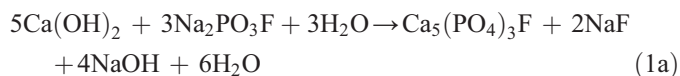
- Influence of high alkalinity (pH≈13) in the pore solution: OH[−] ions and Na⁺ and K⁺ counterions present in the concrete pore network;
- Influence of portlandite Ca(OH)₂, which is another compound influencing concrete alkalinity;
- Influence of CaCO₃ resulting from Ca(OH)₂ carbonation; and
- Influence of the other compounds containing calcium as gypsum (CaSO₄·2H₂O).

For compounds with low solubility (i.e., portlandite (pKs=5.3), calcite (pKs=8.4) and gypsum (pKs=4.6)), the tests consisted of placing these compounds for 24 h in contact with an aqueous solution of 10% MFP by mass. The solid phases were then dried at either 50 or 105 °C (depending on their thermal stabilities) and analysed by means of X-ray diffraction. The filtered solutions were analysed by ion chromatography and atomic spectrometry.

For soluble compounds (KOH and NaOH), the tests consisted in observing the possible formation of a precipitate and analysing the solution by ion chromatography.

Ion chromatograms from the NaOH or KOH solutions showed no interaction between MFP and the alkaline solutions: only the PO₃F^{2−} ion, resulting from MFP dissolution, was observed in the chromatograms.

Concerning Ca(OH)₂, CaCO₃, and CaSO₄ in contact with MFP solutions, it may be stated that if a chemical reaction occurs with apatite formation (Ca₅(PO₄)₃F), the reactions for each of the considered compounds would be:



Consequently, PO₃F^{2−} ions would disappear (due to low apatite solubility) and F[−] ions appear (soluble NaF) within the liquid phase. Under stoichiometric conditions and after a 24-h contact period, the ion chromatograms derived on the solutions (see Fig. 1a, b and c) indicate that just the portlandite had reacted.

This result was confirmed by X-ray diffraction: a new solid phase appeared only with portlandite, which was identified as apatite (Fig. 2).

Taking into account the similarity of X-ray diffraction spectra for fluoroapatite (card ICDD 15-876) and hydroxy-

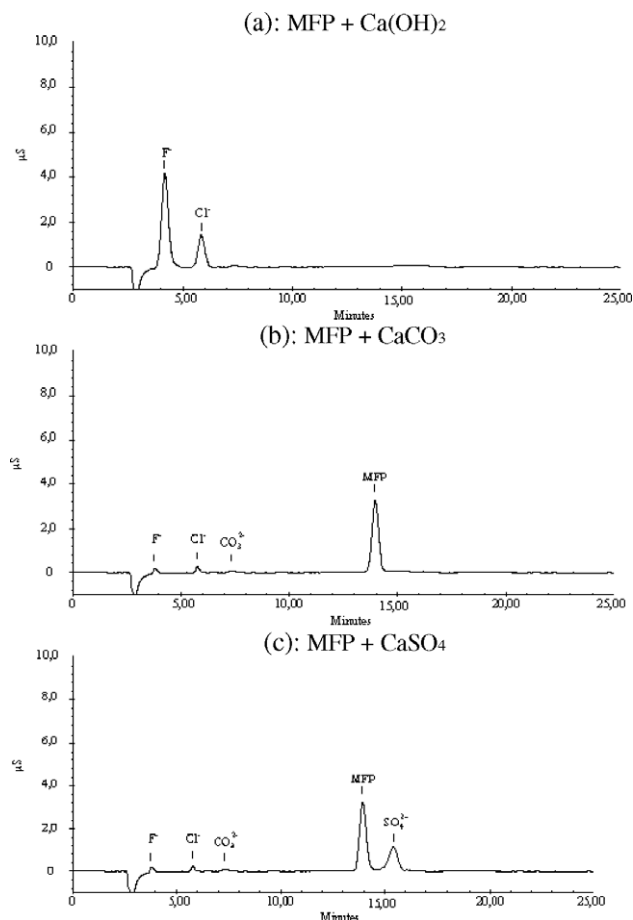


Fig. 1. Ion chromatograms for filtrated solutions after 24 h contact of MFP and CaX (with $X=(\text{OH})_2$ (a), CO_3 (b) or SO_4 (c)) in aqueous solutions.

apatite (card ICDD 9-432), the solid phase, resulting from contact between Ca(OH)_2 and the aqueous MFP solution, was analysed by means of ion chromatography and atomic spectrometry after total nitric acid attack. Both the P/F and Ca/P molar ratios obtained (3.32 and 1.64, respectively) led to conclude that fluoroapatite was indeed the reaction product (for $\text{Ca}_5(\text{PO}_4)_3\text{F}$, P/F=3 and Ca/P=1.66).

3.2. Influence of chloride ions on apatite formation

Considering the formation of insoluble fluoroapatite ($K_s=3.16 \cdot 10^{-60}$) when Ca(OH)_2 is present, the two main consequences to be expected as regards corrosion protection were: the limited penetration of chloride ions due to a reduction in pore size, and the entrapment of chloride ions in the form of another variety of apatite, namely chloroapatite ($\text{Ca}_5(\text{PO}_4)_3\text{Cl}$), which is also highly insoluble.

The effect of reducing the pore network has not been studied herein. Concerning chloride ion entrapment, the same type of experiment as previously presented was carried out by simultaneously adding sodium chloride to the mixture of portlandite and MFP. X-ray diffraction of the precipitated solid phase led to recognition that in this case, fluoroapatite was also being formed. Chloride ion determination in the liquid phase has confirmed that these ions did not participate in the reaction.

3.3. MFP penetration profiles in hardened cement pastes

Using a dedicated method for determining the amount of MFP in cementitious materials [6], MFP penetration profiles in carbonated or non-carbonated hardened cement pastes were determined. These profiles were obtained 7 and 28 days after application of MFP aqueous solution on the surface of cement paste specimens.

A 5-mL volume of an aqueous MFP solution (20% by mass) was applied to one of the surfaces perpendicular to the axis of cylindrical cement paste specimens (3 cm diameter, 6 cm high), either carbonated or not. Adhesive aluminium foils were used to seal all other surfaces.

Following MFP solution application, the specimens were maintained at a relative humidity of 55% and a temperature of 20 °C. This level of relative humidity was chosen in order to facilitate MFP penetration within the hardened cement paste specimens by drying the face on which the MFP solution is applied. In order to facilitate MFP diffusion by wetting/drying cycles, the specimens used for the 28-day testing period were, in addition, submitted each week to a 5-mL volume water application on the specimen surface.

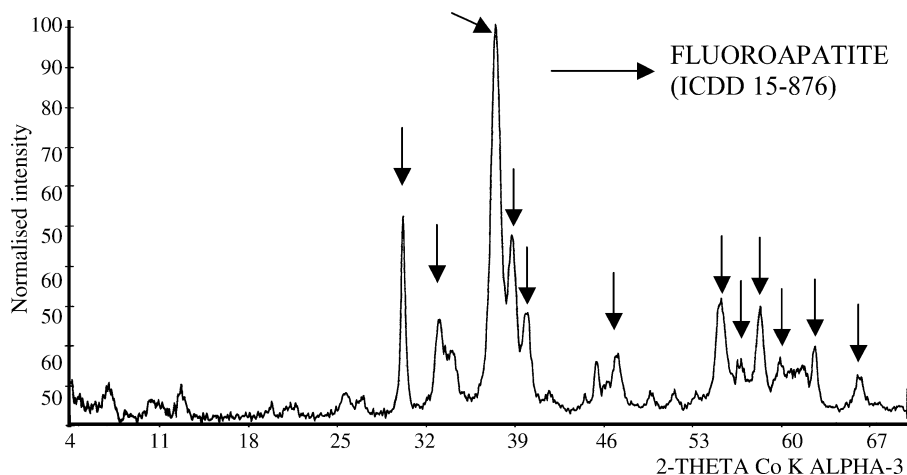


Fig. 2. X-ray diffraction spectrum for the solid phase obtained after contact between Ca(OH)_2 and MFP aqueous solution.

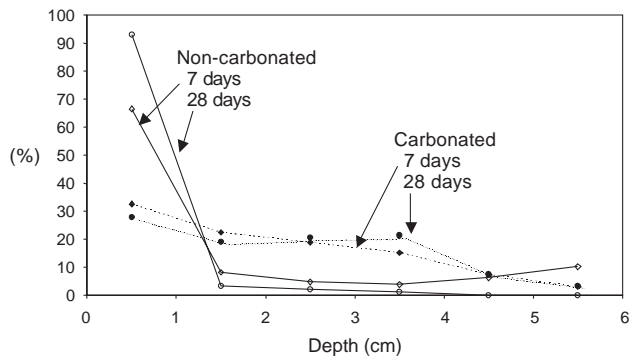


Fig. 3. MFP penetration profiles (determined MFP / total applied MFP in %) in carbonated or not carbonated hardened cement pastes.

The MFP penetration profiles in hardened cement pastes, both carbonated and not, are presented in Fig. 3.

The MFP penetration profiles proved to be very different depending on the state of the hardened cement pastes, but no notable differences have been observed between the two contact durations.

In the non-carbonated cement pastes, the MFP remains mainly within the first centimetre from the surface of application. MFP penetration has been slowed due to the fact that this compound reacted with portlandite to form fluoroapatite. However, MFP at low content levels (only 0% to 10% of MFP applied) was found at greater depths as a result of initial capillary penetration, yet this is unlikely to be effective against steel corrosion given that it only appeared in the form of non-soluble apatite.

In carbonated cement pastes, MFP was distributed uniformly throughout the depth. The presence of CaCO_3 (instead of Ca(OH)_2) has made it possible for MFP to penetrate, with no interaction being observed between calcite and MFP.

3.4. Validation on reinforced mortar specimens

By taking account of the fact that MFP can penetrate into both carbonated cementitious materials in the form of PO_3F^{2-}

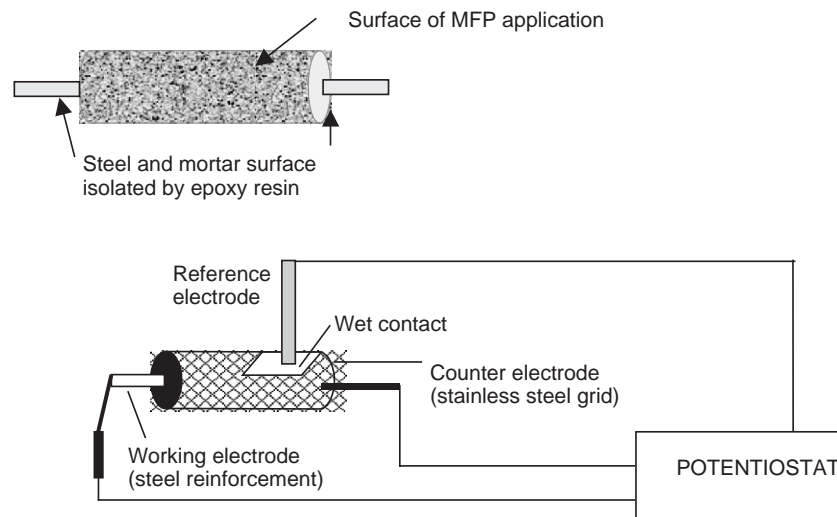


Fig. 4. Mortar samples for electrochemical tests.

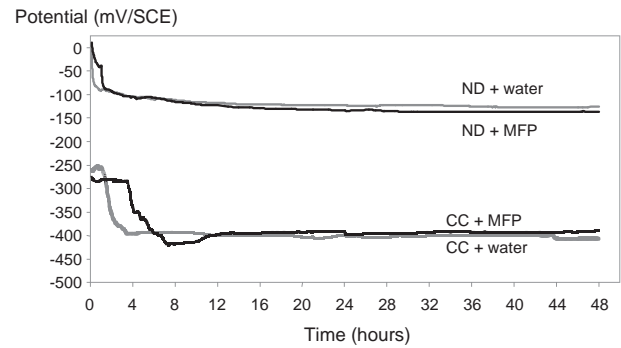


Fig. 5. Evolution of the steel corrosion potential after applying MFP solution or water onto reinforced mortar surface (non-carbonated mortars) (ND: non-degraded – CC: chloride contaminated).

ions and non-carbonated cementitious materials by capillary action before precipitation in the form of insoluble fluoroapatite through reaction with portlandite, MFP solutions (10% by mass) were applied onto the surface of mortar specimens with steel reinforcements positioned at 1.4 cm from the surface (see Fig. 4).

With such a small cover depth, the tests showed that in all cases, MFP reached the steel surface. The objective then was to determine the inhibitor effect of MFP present in various forms (apatite or ions). To correlate the results obtained with MFP solutions, tests were also conducted with water. In all cases, the volume (water or MFP solution) applied onto the mortar surface was set equal to 10 mL. The determination of MFP effectiveness was carried out by means of electrochemical tests.

Before running the experiments, some mortar specimens were submitted to chemical degradations, i.e.:

- No degradation (ND),
- Total carbonation (TC),
- Contamination by chlorides (0.5% to 0.8% of Cl^- in the mortar close to the steel bar) (CC), and
- Total carbonation and contamination by chlorides (TC+CC).

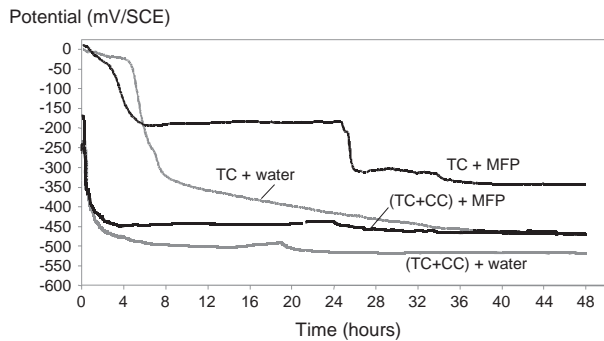


Fig. 6. Evolution of the steel corrosion potential after applying MFP solution or water onto reinforced mortar surface (carbonated mortars) (TC: total carbonation – CC: chloride contaminated).

The monitoring of steel corrosion potential in the mortar specimens was performed upon application of the MFP solution for a period of 48 h.

The $E=f(t)$ curves obtained following application of water or MFP solution on non-carbonated mortars (ND and CC) revealed no particular effect from MFP (see Fig. 5); these curves, based on the initial potential, showed that potential was constant over a certain time and then a rapid decrease (100 to 150 mV_{SCE}) appeared. At the end of this decrease, the potential once again remained constant. The abrupt drop in potential observed after a few hours (2 h in the absence of chlorides, and 4 to 6 h when chlorides were involved) clearly characterises the access of the aqueous phase to the steel surface. No effect ascribable to the action of MFP was observed on the steel corrosion, although the inhibitor was found quite near to the steel surface (2% to 9% of the applied MFP was identified after total dissolution of the mortar in nitric acid). This finding was simply due to the absence of free MFP ions, resulting from their reactivity with portlandite in a non-carbonated mortar.

With regard to the delayed times at which the potential decreases occurred in the presence of chlorides, it is possible that adsorption of chloride ions on the pore walls led to limit the diffusion of aqueous solutions.

The $E=f(t)$ curves obtained after application of water or MFP solution on carbonated mortars are presented in Fig. 6. The overall shape of these curves is very similar to that of the previous ones with non-carbonated mortar: the potential remained constant over a certain period prior to the appearance of a rapid decrease (100 to 150 mV_{SCE}), subsequent to which the potential remained constant once again. Differences have been observed however between the two sets of curves that help highlight the effect of MFP at the steel surface. First of all, it should be noted that the latency time representing the diffusion of water into mortars is higher for the non-chlorinated mortar, whereas this time falls to nearly zero for the chlorinated mortar regardless of the presence or absence of MFP. It is possible that the hygroscopic property of chlorides present in the pores and not adsorbed when the mortar was carbonated has facilitated the diffusion of water within the porosity [10–12]. The major difference in the case of carbonated mortars is that in the presence of MFP, the potential curves are significantly modified in comparison with those obtained in the absence of MFP: the potentials reached in the presence of MFP are more positive. The most significant curve was that generated in the absence of chloride ions within the mortar. In contrast with the absence of MFP in the water applied to the carbonated mortar surface, for which the potential decreased in a monotonous manner as a function of the time required for stabilization towards –450 mV/ECS; in the presence of MFP, the potential stage reached after 5 h of contact was definitely higher, located at –190 mV/ECS. This is related to the main anodic effect of the inhibitor at low concentration. After 24 h of the test period had elapsed, a second potential drop was observed; this one was both abrupt and significant (amplitude of 100 mV), but the final potential still remained more highly positive than that measured in the absence of MFP. This second drop in potential was probably related to an increase in the concentration of MFP within the zone close to the metal surface [5]. In this case the inhibitor effect becomes mainly cathodic. In the presence of chloride ions within the carbonated mortar, the $E=f(t)$ curves obtained indicated the same

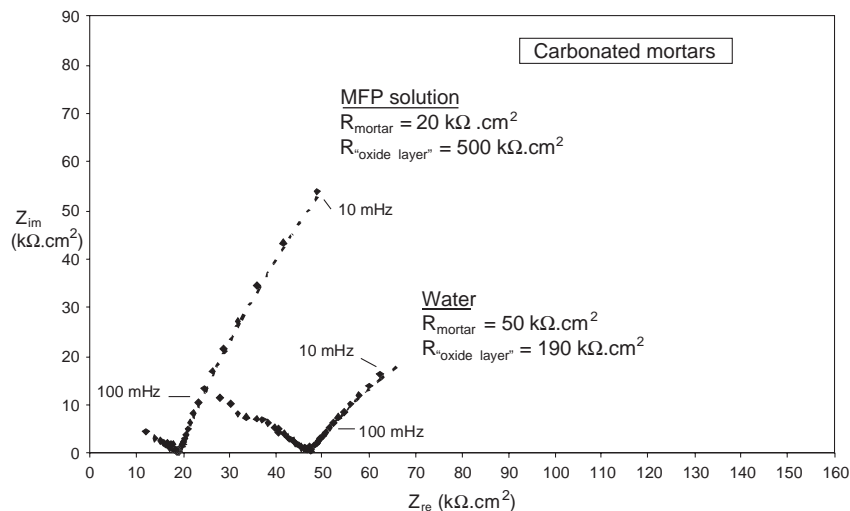


Fig. 7. EIS diagrams for carbonated mortars 48 h after application of aqueous solutions (MFP or water).

characteristics as in the absence of chloride, yet in a less distinct manner.

Electrochemical impedance spectroscopy measurements were also conducted 48 h following application of the aqueous solutions on mortar surfaces. Fig. 7 presents some of the EIS diagrams obtained on carbonated mortars. The experimental data have been modelled using a resistivity/capacitance circuit in order to derive information on the mortar and steel/mortar interface: the high-frequency response corresponds to the bulk concrete, while a medium-to low-frequency response corresponds to passivation or corrosion processes at the steel/mortar interface, as acknowledged by some authors [7,13,14]. The EIS measurement results obtained in this study have not enabled estimation of corrosion rate of steel in contact with the mortar, but nonetheless the following can be observed (see the values shown in Fig. 7):

- Mortar resistivity decreased when MFP was present (50 to 20 $\text{k}\Omega \text{ cm}^2$); and
- MFP exerted a passivating effect on the steel surface, as the “oxide” layer resistivity increased from 190 to 500 $\text{k}\Omega \text{ cm}^2$.

4. Conclusion

In this study on MFP used as a concrete reinforcement inhibitor, an interaction between MFP and calcium ions has been highlighted, when the portlandite $\text{Ca}(\text{OH})_2$ is present but not in the presence of other Ca-containing compounds such as calcium carbonate CaCO_3 . When portlandite was present, the interaction led to the formation of fluoroapatite, which then limited penetration of MFP into the concrete.

The difficulty of penetration of MFP into non-carbonated concrete and thus inhibiting the corrosion process was confirmed by corrosion potential measurements on steel in mortars during the 48 h following MFP application on the mortar surface.

In the case of a carbonated cementitious material, MFP is able to penetrate. Under laboratory conditions, chemical analyses on carbonated cement pastes have shown that MFP ions could reach a depth of 40 mm. Electrochemical measurements performed on steel in carbonated mortars confirm this level of penetration and show that when MFP ions reach the steel surface, they become effective in improving steel protection.

References

- [1] B. Elsener, Corrosion Inhibitors for Steel in Concrete-State of the Art Report, European Federation of Corrosion Publication N° 35, Maney Publishing, London, 2001, 80 pp.
- [2] B. Elsener, R. Cigna, in: Romain Weydert (Ed.), Surface Applied Inhibitors, COST 521 Workshop on Corrosion of Steel in Reinforced Concrete Structures, Luxembourg, Final Report, 2002 (18–19 February), p. 165.
- [3] V.T. Ngala, C.L. Page, M.M. Page, Corrosion Science 45 (2003) 1523.
- [4] A. Raharinaivo, B. Malric, Int. Conf. on Corr. and Rehabilit. of Reinf. Concr. Struct., Orlando, 1998.
- [5] V. Nobel-Pujol Lesueur, Effectiveness of a corrosion inhibitor for steel in concrete: The MFP (in French), PhD dissertation, Pierre et Marie Curie University, Paris VI, 2004, 186 pp.
- [6] F. Farcas, T. Chaussadent, C. Fiaud, I. Mabilie, Analytica Chimica Acta 472 (2002) 37.
- [7] V. Feliu, J.A. Gonzales, C. Andrade, S. Feliu, Corrosion Science 40 (1998) 995.
- [8] C. Andrade, V.M. Blanco, A. Collazo, M. Keddah, X.R. Nóvoa, H. Takenouti, Electrochimica Acta 44 (1999) 4313.
- [9] G. Trabanelli, C. Monticelli, V. Grassi, A. Frignani, Cement and Concrete Research 35 (2005) 1804.
- [10] L.J. Parrott, Cement and Concrete Research 22 (1992) 1077.
- [11] W.P.S. Dias, Cement and Concrete Research 30 (2000) 1255.
- [12] L. Basheer, J. Kropp, D.J. Cleland, Construction and Building Materials 15 (2001) 93.
- [13] L. Hachani, C. Fiaud, E. Triki, A. Raharinaivo, British Corrosion Journal 29 (1994) 122.
- [14] A.A. Sagues, S.C. Krac, E.I. Moreno, Corrosion Science 37 (1995) 1097.